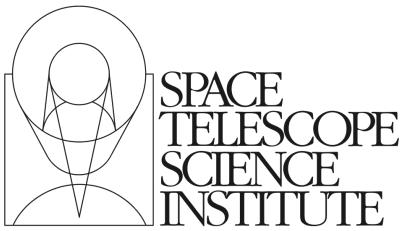

Instrument Science Report WFPC2 2009-003

Pipeline Correction of Images Impacted by the WF4 Anomaly

V. Dixon and J. Biretta
April 30, 2009

ABSTRACT

The WF4 CCD anomaly is characterized by low or zero CCD bias levels, lowered count levels on the WF4 detector (i.e., low CCD gain), and faint horizontal background streaks. To correct the first two effects, a new processing step has been added to the WFPC2 calibration pipeline. It rescales each pixel using a gain correction that depends on the observed pixel value and the bias level of the image. Internal VISFLAT observations have been used to derive the corrections, which are tabulated into separate reference files for gain 7 and gain 15 data. After correction, the WF4 images show normal bias levels. Photometric tests using the standard star GRW+70D5824 indicate that the corrections are generally accurate to ~ 0.01 magnitude, with lower accuracy of ~ 0.02 magnitude in some infrequent cases. In most cases, the photometric properties of the corrected WF4 images are essentially indistinguisable from normal images taken in the other WFPC2 CCDs.

Introduction

Since early 2002, the WF4 detector of the Wide Field Planetary Camera 2 (WFPC2) has exhibited an anomaly characterized by low or zero bias levels, faint horizontal streaks, and low count levels (Biretta and Gonzaga 2005). The problem is thought to be caused by a failing amplifier in the WF4 signal-processing electronics. The anomaly is temperature dependent and since January 2006 has been mitigated by reducing the

Operated by the Association of Universities for Research in Astronomy, Inc., for the National Aeronautics and Space Administration

temperature of the instrument at regular intervals (Dixon et al. 2007). To correct for the effects of the anomaly, a WF4 gain-correction step has been added to the WFPC2 data-reduction pipeline (specifically, to the CALWP2 software). It rescales the counts in each pixel (also called digital numbers or DN), correcting the photometry and restoring the bias to its normal level. In this ISR, we describe the algorithm, the construction of its reference files, and its efficacy. A second routine, described by Maybhate et al. (2008), has been developed to remove the faint horizontal streaks seen in some low-bias images.

Construction of the Reference Files

Ideally, the gain correction would be derived from a set of images of a single target that spans the full range of pixel values (0 to 4095) and bias levels (0 to ~ 310), including several reference images with normal bias levels. (The normal bias levels are approximately 311 and 305 DN, respectively, for A/D gain settings of 7 and 15.) For this purpose we used internal flat-field (VISFLAT) images, which have the advantage of not requiring pointed HST time and being generally immune to CTE effects. The internal flat-field images used are listed in Tables 1 and 2. Unfortunately, these images are not always identical, even for a single filter and shutter combination: the WFPC2 filter wheel may not position the filter at the same spot for each exposure (Gonzaga et al. 2002), so finding a reference image appropriate for a particular low-bias image requires some trial and error. Neither do the images span the full range of bias levels: the bias level cannot be set, but instead fluctuates on short time scales in response to the camera temperature. Hence we must interpolate (and sometimes extrapolate) to fill parameter space. Finally, for some filters, no images with normal bias levels are available, and we must construct reference images using information from other filters. Nevertheless, we have been able to construct reliable reference files for A/D gains of 7 and 15, as described below.

Table 1. Flat-Field Images Used to Construct Reference Files for Gain 7 Data

Filter	Exposure Time (s)	Shutter	Proposal IDs	Number of Images	Bias Range	DN Range
F555W	18	A	10779, 11030	88	24-309	1500-2500
F555W	30	A	10777	4	20, 254	2500-4100
F555W	30	B	10779, 11030	145	87-309	2500-4100
FR868N18	10	B	8942, 9597, 10075, 10363, 10772, 11029	42	1-225, 290-311	315-1800

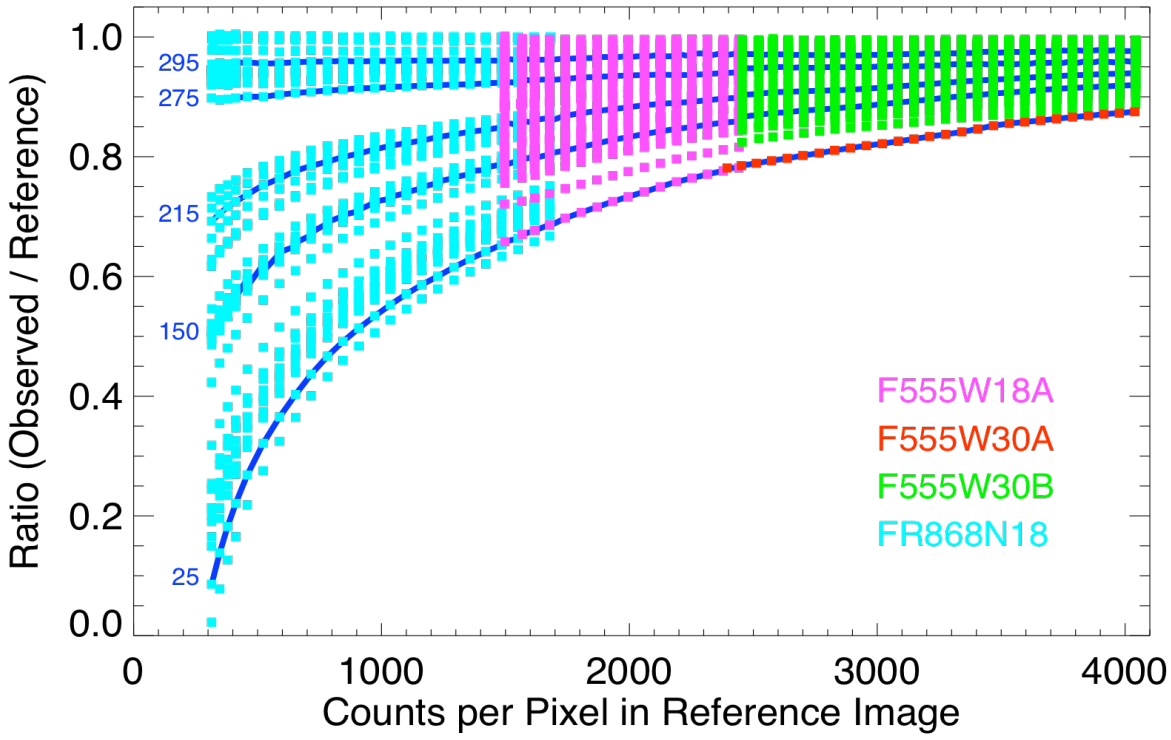

Figure 1. The ratio (observed median) / (reference median) as a function of the counts per pixel in the reference image for the gain 7 data. The points are color coded according to the filter, exposure time, and shutter listed in Table 1. The dark blue lines trace the observed/reference ratio for the indicated bias values.

Gain 7 Reference File

To construct a reference file for the gain 7 data, we begin with 42 internal flats obtained through the FR868N18 filter (Table 1). This rotated linear ramp filter has the property that an extremely wide range of illumination, extending down to zero light, occurs in the WF4 field of view. Four images have bias values of ~ 311 DN. We use one of them, U6I27I02M, as a reference. Considering only the central 500 × 500 pixels, we identify all pixels with values in the range 300-331 DN (there are no fainter pixels in this high-bias image), record their positions on the chip, and compute their median value. For each of the 42 individual images, we then identify the same pixels, compute their median value, and compute the ratio (observed median) / (reference median). We repeat the process for DN ranges 332-364, 365-396, etc. For the gain 7 files, our first four bins are 32 DN wide; subsequent bins are 64 DN wide. For the gain 15 files, all bins are 64 DN wide. Bins containing fewer than 30 pixels are ignored.

Figure 1 shows a plot of the observed/reference ratio as a function of the counts per pixel in the reference image for the entire gain 7 data set. The cyan points represent data obtained through the FR868N18 filter. We will discuss the data from the other filters in a moment, but first let us consider the general features of the plot. The points from a single

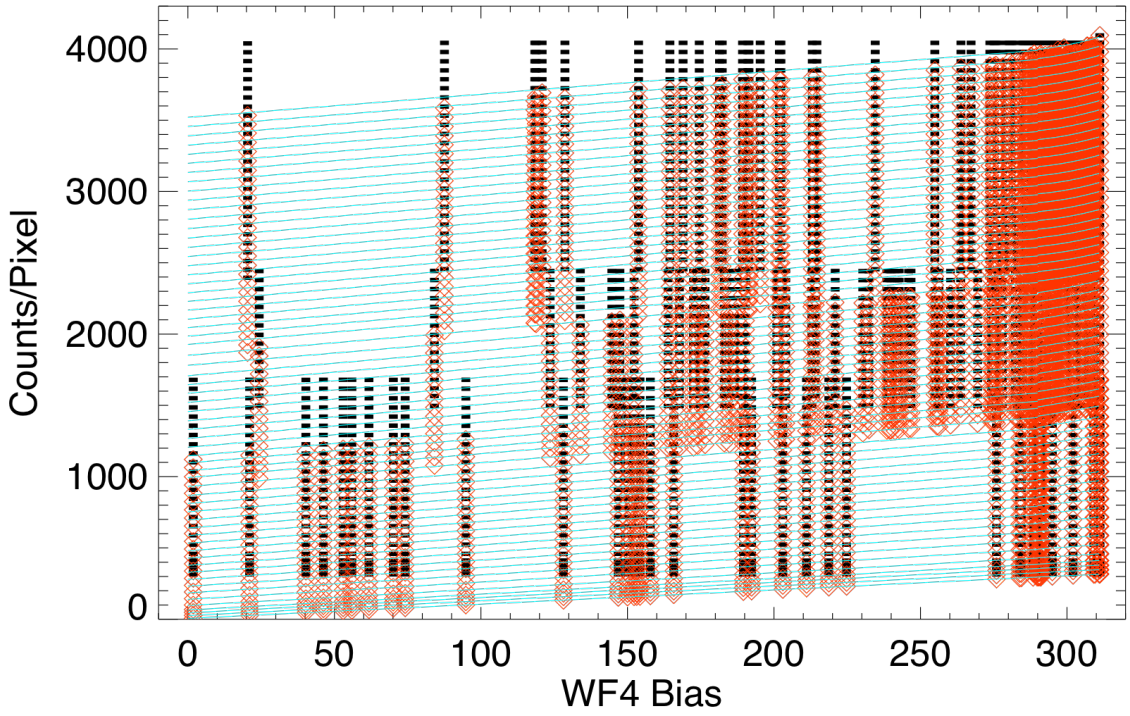

Figure 2. Observed and reference counts as a function of the bias level for the gain 7 data. Black bars represent reference values, red diamonds represent observed values, and cyan curves are polynomial fits to the observed values. All of the data points from Fig. 1 are included on this plot.

image form an arc from lower left to upper right across the figure. For high-bias images, the observed/reference ratio is nearly flat and close to unity. For low-bias images, the observed/reference ratio is a steep function of the reference counts.

With this pattern in mind, we can populate the rest of the figure using standard F555W VISFLATs, which have nearly uniform illumination across the WF4 CCD. The 18-second F555W images have bias values between 24 and 309 DN. To construct a bias = 311 reference image, we use the FR868N18 data to determine the correction appropriate for an image with a bias of 309. Because the observed/reference ratio is independent of pixel value for high-bias frames, a uniform multiplicative correction is sufficient. Using this reference image, we compute observed/reference ratios for the other images in this filter set. They are plotted as magenta points in Fig. 1.

The 30-second F555W images obtained using shutter B have bias values ranging from 87 to 309. Again, we construct a reference image by scaling a bias 309 image to an effective bias of 311 and use it to compute observed/reference ratios for this filter set. The results are plotted in green in Fig. 1.

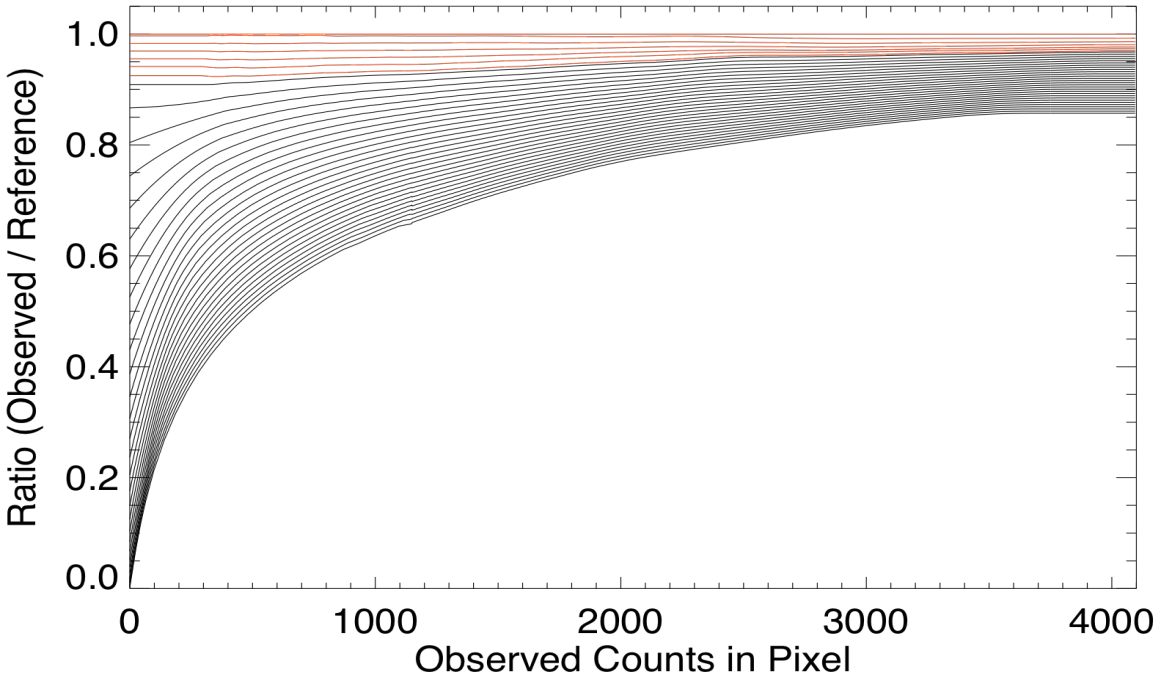

Figure 3. The predicted ratio (observed counts) / (reference counts) as a function of observed counts for the gain 7 data. Black curves represent bias values between 10 and 280 (in steps of 10); red curves represent bias values between 285 and 310 (in steps of 5) plus 311.

Finally, to extend our data set into the low-bias, high-DN regime, we use four 30-second F555W images obtained using shutter A. Three have bias values near 254, and one has a bias of 20. For bias values as low as 254, the gain correction is no longer independent of the pixel value, so we construct a draft reference file (as described below), apply it to the three bias = 254 images, and combine them (using a median filter) to construct a reference image. The reference image is then used to compute the observed/reference ratios plotted in red in Fig. 1.

Early versions of Fig. 1 showed that the observed/reference ratios derived from the 18-second F555W images (magenta points) differed by a couple of percent from those derived from the other filters in the regions of overlap. To correct this discrepancy, we rescaled the magenta points using a second-order polynomial. The corrected ratios vary smoothly with pixel value, as can be seen in the dark blue lines, which trace the observed/reference ratio for bias values ranging from 25 to 295.

One could construct a reference file directly from Fig. 1, but the curves for individual bias values are not well fit by simple polynomials, and the best way to interpolate between observed bias values – or to extrapolate beyond them – is unclear. A simpler and more robust technique is illustrated in Fig. 2, where we plot (as red diamonds) the observed pixel value as a function of bias level for each of the images shown in Fig. 1. Black bars show the corresponding counts in the reference image. Cyan curves connect

the observed count levels that correspond to each reference count level. (We fit one second-order polynomial to the bias values less than 295 and another to the values greater than 285.) For bias levels less than 290, the curves are nearly linear with a slope close to unity. For bias levels greater than 290, the second-order term becomes important.

We interpolate between these curves to construct a reference file valid for all bias and pixel values. The reference file is essentially a two-dimensional lookup table with axes of "observed pixel value" and "observed bias value" in which each cell gives the value of the multiplicative correction. The correction is stored as an image with dimensions 4096 (pixel value) by 350 (bias value). For a particular WF4 image, the pipeline interpolates between the tabulated (integer) bias values to produce a one-dimensional 4096-element correction array. For each pixel in the image, it interpolates between the tabulated (integer) pixel values to determine the correction for the observed pixel value. Selected slices of the correction image (actually its inverse) are plotted in Fig. 3, which is essentially a fit to the data in Fig. 1, though plotted against observed rather than reference counts.

Gain 15 Reference File

To construct a reference file for the gain 15 data, we begin with the 20-second exposures obtained through the F555W filter (Table 2). This filter set includes four images with the normal bias value (304.6 DN), three from 2004 and one from 2008. We combine all four into a single reference image using a median filter and generate a set of observed/ reference ratios as described above. For about a third of the files, we use only the 2008 high-bias frame as a reference image. The resulting ratios are plotted in cyan in Fig. 4.

To compute observed/reference ratios for higher DN values, we use F555W exposures of 36 and 60 seconds duration (Table 2). In both filter sets, the maximum bias level is 0.5 to 1 DN below the normal value, so we rescale the reference frame, assuming that the correction is independent of DN as described above. The resulting ratios are plotted as green and red points in Fig. 4.

Table 2. Flat-Field Images Used to Construct Reference Files for Gain 15 Data

Filter	Exposure Time (s)	Shutter	Proposal IDs	Number of Images	Bias Range	DN Range
F555W	20	B	10067, 10072, 10356, 10360, 10744, 10745, 10777, 11030	28	7-305	300-1800
F555W	36	A	10777, 10779, 11030	18	11-303	1600-2600
F555W	60	A	11030	24	286-304	2500-4100
FR868N18	20	A	10772	19	1-293	300-3300
FR868N18	20	B	10772	14	4-293	300-3300

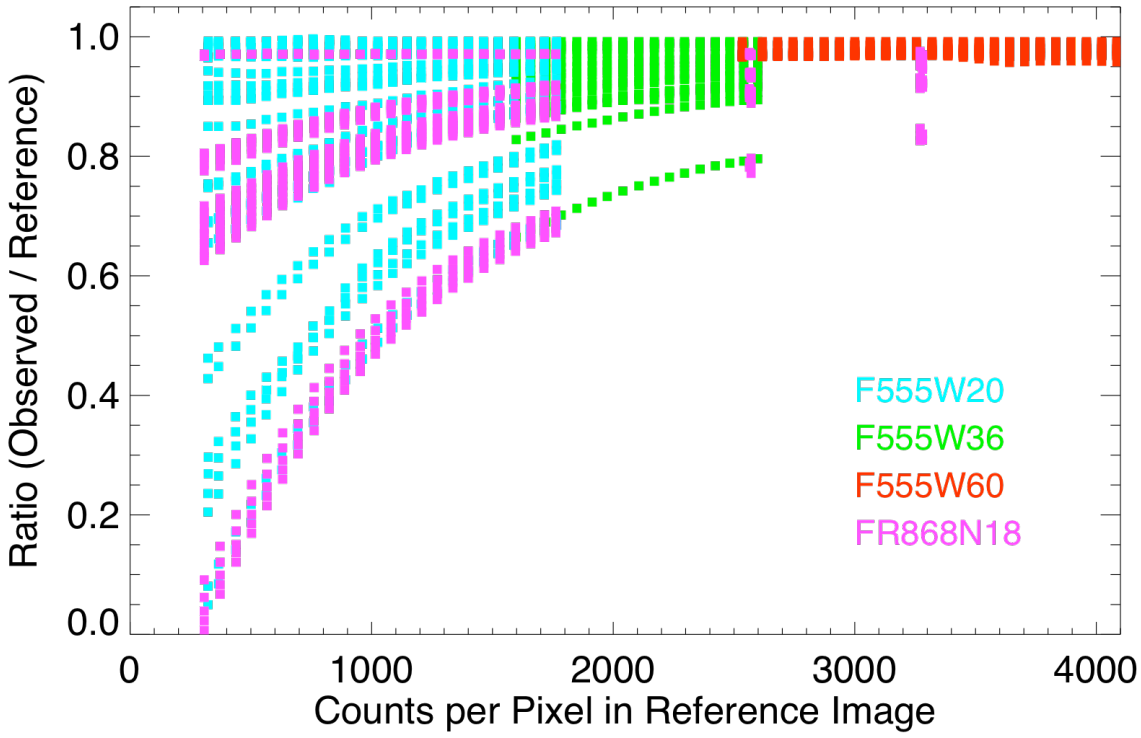

Figure 4. The ratio (observed median) / (reference median) as a function of the counts per pixel in the reference image for the gain 15 data. The points are color coded according to the filter and exposure time listed in Table 2.

To extend the plot to lower bias values, we include data obtained through the FR868N18 filter using both shutters A and B. For each shutter, we construct a reference image by combining three high-bias frames using a median filter. In this case, "high bias" means 293 DN, so we must scale both reference images by approximately 1.03 to reproduce a normal-bias image. Fortunately, a bias of 293 is high enough that the correction is nearly independent of DN. The resulting ratios are plotted in magenta in Fig. 4.

Note the two magenta stripes at DN values of approximately 2600 and 3300 in Fig. 4. They represent pixels from column 800 on the WF4 detector. In order to sample the low-bias, high DN region of parameter space, we use the entire image, not just the central region, from the FR868N18 filter set. Pixels from this filter were chosen because the resulting observed/reference ratios match those of the F555W frames in the regions of overlap.

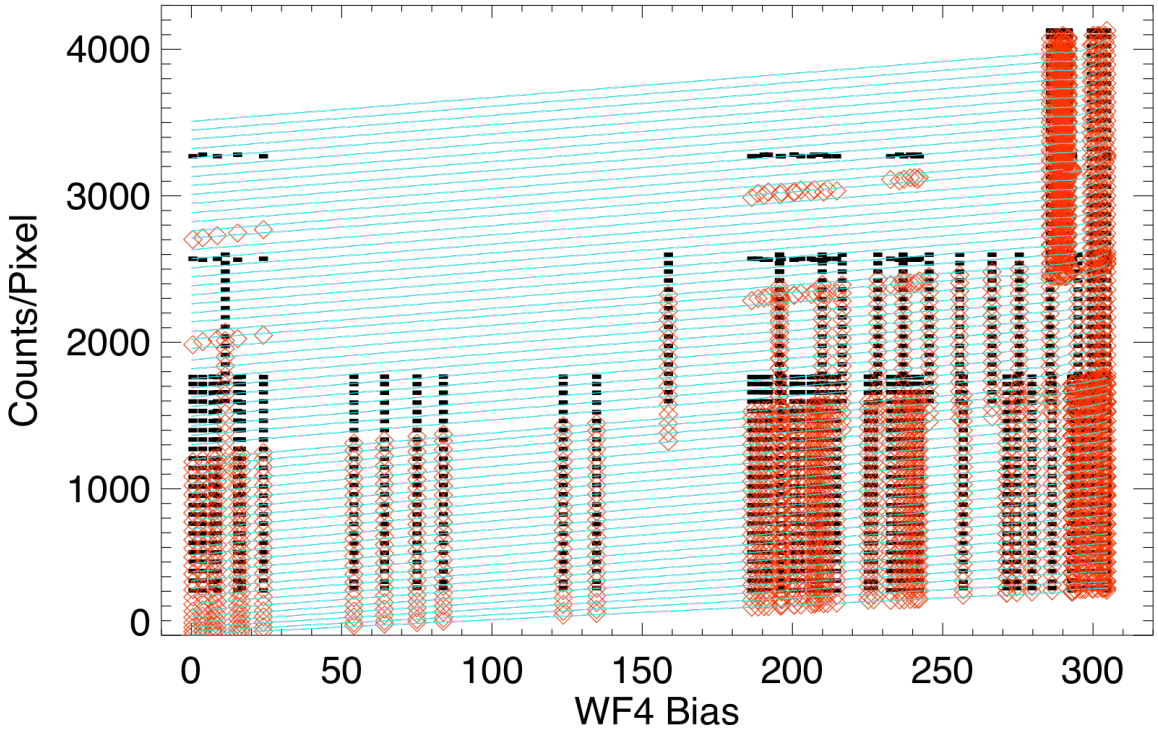

Figure 5. Observed and reference counts as a function of the bias level for the gain 15 data. Black bars represent reference values, red diamonds represent observed values, and cyan curves are polynomial fits to the observed values. In the upper portion of the plot, the curves are linear with a fixed slope. All of the data points from Fig. 4 are included on this plot.

As we did for the gain 7 data, we plot in Fig. 5 the gain 15 results as a function of the bias value. The observed pixel values are shown as red diamonds, black bars show the corresponding counts in the reference image, and cyan curves connect the observed counts that correspond to each reference count level. The dearth of low-bias, high DN data is particularly apparent in this diagram. For this region of parameter space, we adopt a linear fit, fix the slope to be 1.63 (a value derived from the one row of data that is available), and adjust the Y-intercept to match the available high-bias data. The slope is consistent with the value obtained by fitting the gain 7 data with a linear function. From the cyan curves in Fig. 5, a reference file is derived just as for the gain 7 data.

Comparing the Gain 7 and 15 Corrections

Our limited knowledge of the WF4 anomaly and related electronic components prevents a meaningful comparison of the gain 7 and 15 reference files. The electronics failure responsible for the WF4 anomaly is probably located ahead of the A-to-D converters, reducing the input signal below their calibrated linear range (300-4095 DN). As a result, deriving a quantitative relationship between the gain 7 and 15 corrections

may be difficult, if not impossible. The difficulty would be further compounded if the failure affects the analog pre-amplifiers in the gain 7 and 15 channels in different ways. For these reasons, we feel that a detailed comparison of the gain 7 and 15 corrections is not warranted.

Applying the WF4 Gain Correction

The processing and calibration of WFPC2 data are discussed in Chapter 3 of the *HST* WFPC2 Data Handbook (Baggett et al. 2002). Section 3.3 of that document describes the various calibration steps in the pipeline, including the use of header keywords to switch individual steps on and off and to record the names of reference files. To correct the low bias values and photometric errors that characterize the WF4 anomaly, we have inserted a new calibration step, the WF4 gain correction, between the analog-to-digital correction and the bias subtraction. This calibration step is controlled by two new file-header keywords, WF4TCORR, which is set to either PERFORM or OMIT the new calibration step, and WF4TFILE, which records the name of the appropriate reference file (s8q14446u.r7h for gain 7 data and t1l1646du.r7h for gain 15 data). If the keyword WF4TCORR is not present in the data file header, then the new calibration step is not performed.

The WF4 gain correction performs a number of tasks: First, it uses the contents of the .x0h file (overscan columns) to compute the bias level of the uncorrected image, storing the uncorrected values in the new header keywords BIASEVNU and BIASODDU (identical to the calculation of the BIASEVEN and BIASODD keywords in the other CCDs). Second, it rescales the counts in each detector pixel by a correction factor (read from the reference file) that depends on both BIASEVNU and the observed counts in that pixel. Third, it sets a data-quality flag (2048 or bit number 11) for all pixels in images whose bias values are so low that they are unlikely to be properly corrected; this minimum bias value is read from the LOWBLEV keyword of the reference file. By default, this value is 10 DN[1].

We have also modified the bias-subtraction routine: if WF4TCORR = PERFORM, it applies the WF4 gain correction to the contents of the .x0h file before using it to compute the corrected bias level. The resulting bias values BIASEVEN and BIASODD, computed after correction of the .x0h file, are written to the data file header and subtracted from the rescaled image in much the same way as for the other CCDs.

The WF4 gain correction has been incorporated into the MAST version of the calwp2 pipeline, so data retrieved from MAST after August 2008 are corrected for the WF4 anomaly. In particular, all data sets in the static archive are corrected for this effect.

[1] Images with bias level zero are not correctable. For such images, the CCD amplifier offset voltage has fallen below the zero level of the analog-to-digital converter, causing faint pixels to be reported as having zero DN in the raw image. As the bias level approaches zero (bias < 5 DN), the image statistics will be corrupted as more and more pixels become blank.

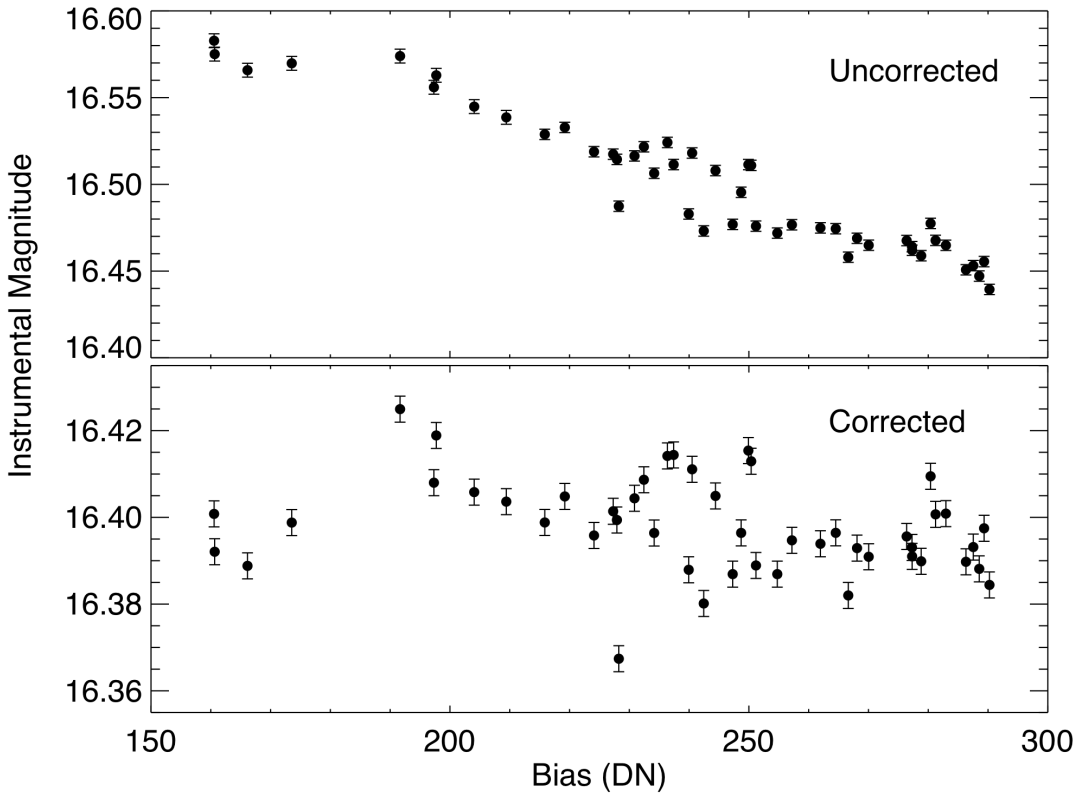

Figure 6. Instrumental magnitudes of the star GRW+70D5824, observed on the WF4 chip with a gain of 7 as part of calibration program 10772. In the upper panel, the data are processed with the WF4 gain correction turned off, and the star appears fainter in low-bias images. In the lower panel, the data are corrected for the WF4 anomaly, and the resulting magnitudes are independent of bias. The standard deviation in the corrected sample is 0.01 mag. Error bars are purely statistical.

Photometric Tests of the Gain Correction

To test the accuracy of the WF4 gain correction, we apply it to observations of the standard star GRW+70D5824, observed with the WF4 chip at a variety of bias levels as part of calibration program 10772 in 2005-2006. These images were obtained in the F555W filter and were typically exposed to a maximum intensity of about 2000 DN per pixel. Figure 6 shows a plot of the star's measured instrumental magnitude as a function of WF4 bias level for bias values ranging from 150 to 300 DN. These data were obtained with a gain of 7. All magnitudes are corrected for time-dependent sensitivity and CTE effects. In the upper panel, the uncorrected data show a clear correlation between stellar magnitude and bias level. In the lower panel, the corrected data yield stellar magnitudes that are nearly independent of the bias. The mean and standard deviation of the magnitudes in the lower panel are 16.398 ± 0.011. The mean is consistent with that of similar observations in the WF3 CCD, 16.412 ± 0.015 mag. The scatter in the corrected

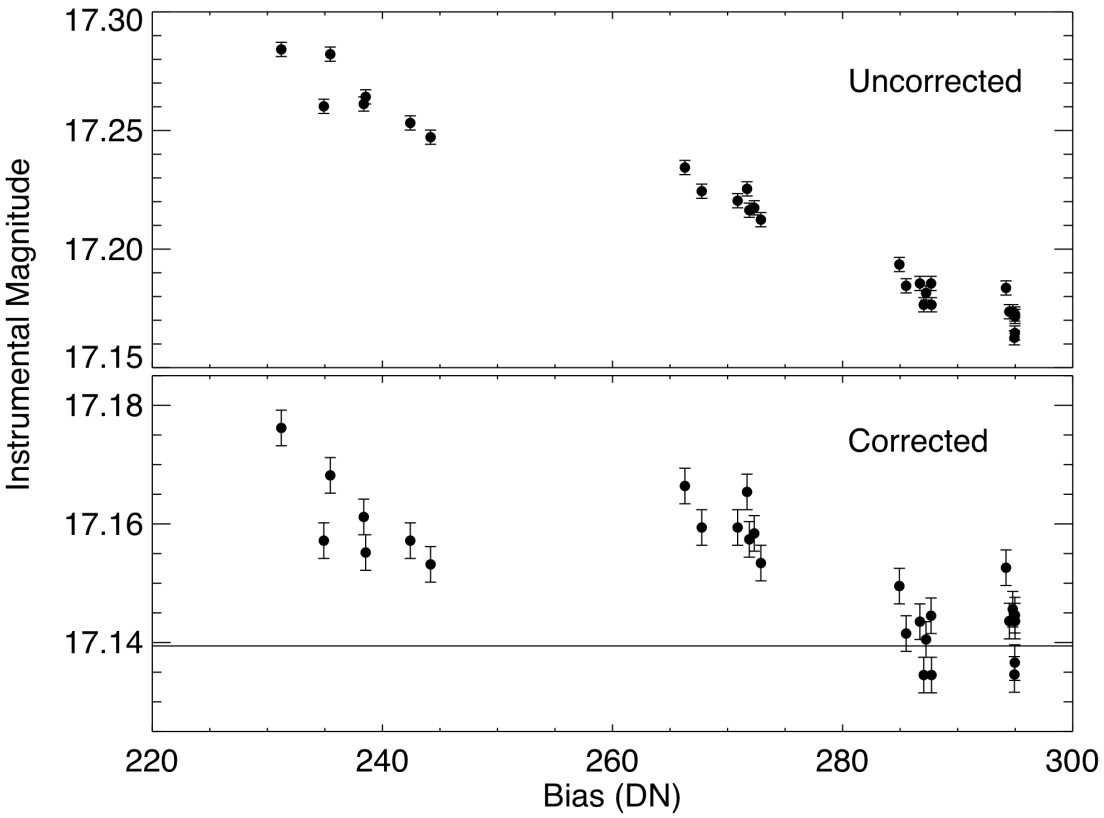

Figure 7. Instrumental magnitudes of the star GRW+70D5824, observed on the WF4 chip with a gain of 15 as part of calibration program 10772. In the upper panel, the data are processed with the WF4 gain correction turned off, and the star appears fainter in low-bias images. In the lower panel, the data are corrected for the WF4 anomaly, and the resulting magnitudes are independent of bias. The solid line represents the magnitude of the same star observed with WF3.

data is due to many effects, including residual CTE errors and flat-field errors, and is similar to the scatter seen for comparable observations made with the other WFPC2 CCDs (~ 0.014 mag). Hence, it appears that the photometry of corrected WF4 images is not significantly degraded by the CCD anomaly.

Plots for gain 15 data are presented in Figure 7. Again, the uncorrected images show a clear dependence of the stellar magnitude on the WF4 bias level, while the gain-corrected images yield magnitudes that are nearly independent of the bias. Three WF3 observations of the same star obtained in 2007 (program 11022) yield a magnitude of 17.139 ± 0.006, represented as a horizontal line. For images with bias levels greater than 280, our corrected images yield a mean stellar magnitude of 17.142 ± 0.006, consistent with the WF3 value. Lower-bias images (bias <280 DN) yield magnitudes that are faint by ~ 0.02 mag. The pixels contributing to the stellar image in these frames populate the low-bias, high-DN region of parameter space – exactly the region for which we have

little calibration data. Fortunately, few low-bias science images were obtained using gain 15. We do not recommend simply subtracting 0.02 mag from all low-bias gain 15 images, because we expect faint pixels (and thus faint stars) on these images to be more accurately corrected.

In principle, it would be useful to have additional standard star (or standard field) tests for fainter images at low bias values; however, in practice this is difficult, because there is little suitable observational material available from the era where the bias values were lowest. In addition, such data would likely suffer from large differences in the CTE properties of the reference epoch and the low-bias epoch, making the WF4 results uncertain.

Conclusions

Using internal flat-field observations through a variety of filters, we have developed reference files and software to correct for CCD gain losses due to the WF4 anomaly. The corrections were tested using images of the standard star GRW+70D5824 and give magnitudes that are independent of bias level. Moreover, the magnitudes and their standard deviations are comparable to those obtained with the other WFPC2 CCDs. For gain 7 images, the scatter in the resulting magnitudes is ~ 0.01 mag, while for gain 15 images with bias values greater than 280 DN, the scatter is ~ 0.006 mag. Low-bias gain 15 images yield standard-star magnitudes ~ 0.02 mag too faint, but this region of parameter space (gain 15, high counts, low bias) has relatively little input data from the VISFLATs and is expected to be less accurate; few science images were obtained with these parameters. Fainter stars in gain 15 low-bias images should be more accurately corrected.

Future Work

Recent analysis has suggested that two effects, neglected in our work to date, may be important. First, the CALWP2 pipeline may systematically under-estimate the bias for images with high backgrounds, particularly the flat-field files (background ~1000 DN) used in this work. Second, the 32- and 64-DN binning used to construct our reference files may be too coarse at low DN levels, resulting in a possible under-correction of pixels with DN levels just above the bias. We will continue to investigate these phenomena and will release new reference files and/or software as appropriate.

Acknowledgements

We would like to thank Luigi Bedin and Katya Verner for their kind assistance with the stellar photometry.

References

Baggett, S., et al. 2002, in HST WFPC2 Data Handbook, v. 4.0, ed. B. Mobasher, Baltimore, STScI

Biretta, J. and Gonzaga, S. 2005, Early Assessment of the WF4 Anomaly (WFPC2 ISR 2005-02).

Dixon, V., Biretta, J., Gonzaga, S., and McMaster, M. 2007, Temperature Reductions to Mitigate the WF4 Anomaly (WFPC2 ISR 2007-01).

Gonzaga, S., Baggett, S., and Biretta, J. 2002, An Analysis of WFPC2 Filter Positional Anomalies (WFPC2 ISR 2002-04).

Maybhate, A., Grumm, D., McMaster, M., and Sirianni, M. 2008, Correcting Background Streaks in WFPC2 Data (WFPC2 ISR 2008-03).